Journal of Imaging Science and Technology® 59(2): 020401-1–020401-10, 2015.

Jetting Frequency and Evaporation Effects on the Measurement Accuracy of Inkjet Droplet Amount

Kye-Si Kwon▲ and Dahai Zhang
Department of Mechanical Engineering, Soonchunhyang University, 22, Soonchunhyang-Ro, Shinchang, Asan Chungnam, 336-745, South Korea
E-mail: kskwon@sch.ac.kr

Hyun-Seok Go
Department of Electrical & Robot Engineering, Soonchunhyang University, 22, Soonchunhyang-Ro, Shinchang, Asan Chungnam, 336-745, South Korea

Abstract. *Inkjet technology has been used as a tool to manufacture printed electronics, and the size of the droplet should be properly measured and controlled in order to improve the print quality. To this end, the volume of an inkjet droplet can be measured by assessing an image of the droplet through the use of a visualization system. However, a vision-based method may have accuracy issues, so, in this study, an alternative method is proposed by using a microbalance to measure the droplet mass. The mass and the volume of the droplet are simultaneously measured for verification and comparison. Since the results of the proposed mass measurement method are susceptible to the evaporation of liquid on the microbalance, the accuracy of the measurement is improved by employing an evaporation compensation method. Finally, the effects of the jetting frequency on the measurement uncertainty of the mass and the volume of the droplet are investigated by using several jetting materials with different boiling temperatures.*

[DOI: 10.2352/J.ImagingSci.Technol.2015.59.2.020401]

INTRODUCTION

The uses for inkjet technology have been expanded beyond home printing, and now such technologies are also used as manufacturing tools. In order to use inkjet printers to manufacture printed electronics, the volume of the droplet produced from the inkjet head should be properly measured and controlled. Vision-based methods have been extensively used to measure the volume of a droplet.[1–4] The accurate measurement of the droplet volume is an important factor to ensure high-quality printing. For example, a multi-nozzle head is often normalized according to the droplet volume that was measured in order to equalize the droplet volume across all nozzles by adjusting the applied drive voltage nozzle by nozzle.[1]

However, vision-based measurements are insufficient in that various image-related errors result in a low accuracy. For example, the lighting conditions and the lens focus may affect the measurements of the size of the droplet. In addition, the results that are measured may differ according to the threshold value that is used, which is required to detect the location of the edges in a grayscale image.[1] To overcome the disadvantages of using vision-based measurements, an alternative droplet mass measurement method has been proposed.[5–7] The droplet mass in the sub-microgram range can be measured using a quartz crystal microbalance and nanomechanical resonators.[6,7] However, such methods require a precise calibration to be performed for specific applications.

This study mainly discusses the gravimetric measurement of the mass of a droplet from an inkjet head by using a commercially available microbalance. Three different approaches have been proposed to correspond to the inkjet jetting modes: burst, continuous, and finite jetting modes.[5] In this study, continuous jetting is discussed for the droplet measurement because the use of a finite number of droplets to measure the mass may have problems in that the first few (or many) droplets are likely to be failure as a result of the ink drying on the surface of the nozzle. In order to use continuous jetting to measure the mass of the droplet, many factors that affect the accuracy of the measurement must be taken into account. For example, the jetting frequency and the evaporation significantly affect the accuracy of the measurements. However, prior research[5] did not discuss the details of such effects. In this work, such effects on mass measurement are investigated by comparing the volume measured for the droplet to that obtained through a vision-based method.

The mass and volume of the droplet are effectively measured by developing an in-situ measurement system. The real-time in-situ mass measurement has a mass measurement interval of 1 s, which is relatively short when compared to the previous method presented in Ref. 5, to plot the mass data with respect to time. By using a real-time plot of the mass, the mass of the droplet can be calculated by the fitting mass data to a linear regression. The use of linear regression has an advantage in that the reliability of the measurement can be verified by investigating the linearity or the coefficient of correlation, which should be more than 0.9. The measured mass is validated by using the jetting image, which was

▲ IS&T Member.

Received Mar. 12, 2015; accepted for publication Apr. 21, 2015; published online May 28, 2015. Associate Editor: Rita Hofmann-Sievert.
1062-3701/2015/59(2)/020401/10/$25.00

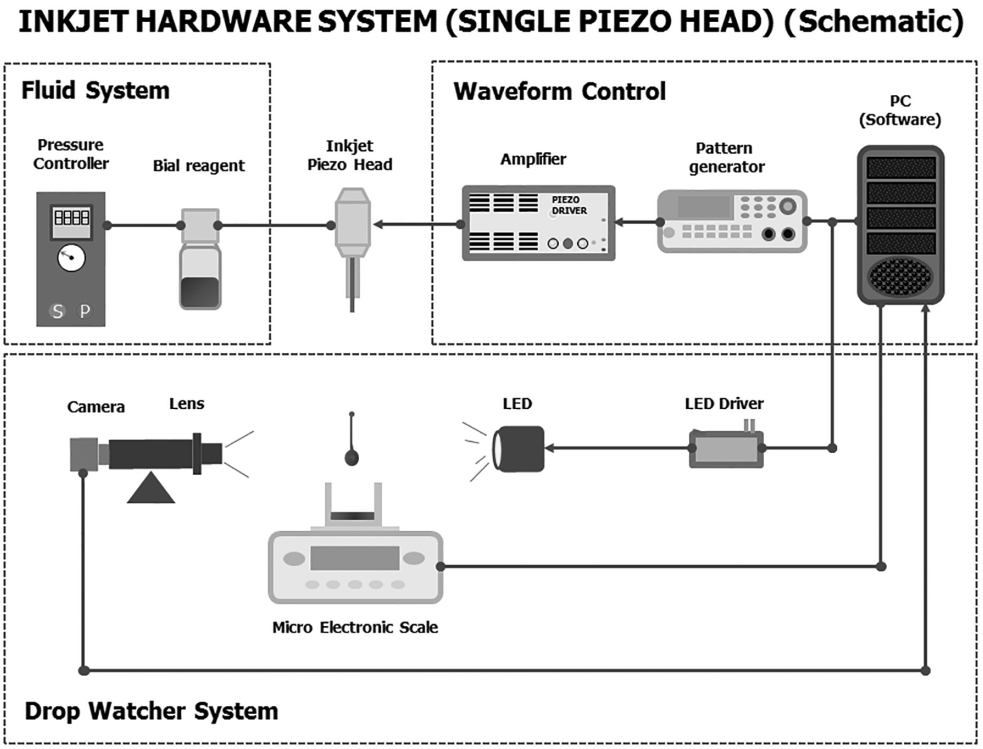

Figure 1. Schematic of the droplet mass measurement and visualization.

simultaneously acquired using a drop visualization system, to obtain the volume of the droplet. Finally, the advantages and disadvantages of using the different droplet mass and volume measurement methods are summarized.

IN-SITU MEASUREMENT METHODS FOR INKJET DROPLET AMOUNT

Experimental Setup

The droplet mass and droplet volume are measured during jetting by using the in-house (laboratory developed) drop visualization and mass measurement system shown in Figure 1. The drop visualization system and the algorithm are described in detail in Refs. 4, 8. In this experiment, a single nozzle head (MJ-AT, Microfab, USA) is used as the jetting device, and the nozzle diameter of the printhead that was used for the experiment was set to 50 μm.

The jetting images are visualized using a CCD camera (STC-TC202USB, Sentech, Japan) to acquire the jet image. An adjustable zoom lens (ML-Z07545, MORITEX, Japan) and a lens adaptor (ML-Z20, MORITEX, Japan) are used to acquire magnified images of the inkjet material. The frozen jetting images are obtained by synchronizing LED lights with the jet triggers.

The mass of the droplet is measured during jetting by using a commercially available microbalance (CPA225D, Sartorius, Germany). The microbalance has a sensitivity of 0.01 mg. The repeatability and linearity are 0.02 mg and 0.03 mg, respectively, but an issue arises in that the measurement resolution is not sufficient to measure the mass of individual inkjet droplet. In addition, the measurement of the mass with the precision microbalance can easily be affected by changes in the measurement environment. Therefore, the total mass of the droplet that is placed on the microbalance should be sufficient for the effects of the environment, such as the humidity and temperature, to be neglected. To this end, a finite number of droplets or continuous jetting with a fixed frequency can be used to place a sufficient amount of droplets on the microbalance.[5] In this study, continuous jetting with a fixed jetting frequency is used for the in-situ measurement of the mass and volume of the droplet. To generate jetting with a continuous frequency, a PCI-6221 counter (National Instrument, USA) is used to trigger the jetting signal. The serial communication of the computer is used to obtain mass data from the balance every second, and the mass data are plotted on graph in real time to obtain the slope of the mass data collected during jetting.

Droplet Volume Measurement

Strobe Light Effects on the Droplet Volume

This section discusses the droplet volume measurement issues for the drop visualization system shown in Fig. 1. A strobe light triggered by the jetting signal was used to obtain a frozen image of the droplet. The brightness of the image can be controlled by adjusting the on-time of the strobe light, T_{on}, as shown in Figure 2. In addition, the brightness of the image is also affected by the jetting frequency when T_{on} of the strobe light is fixed. The duty ratio, defined by T_{on}/T, which ranges from 0 to 1, accounts for the brightness in the image. Here, T is the period of the LED light, which is the inverse of the jetting frequency, f. For example, the images obtained

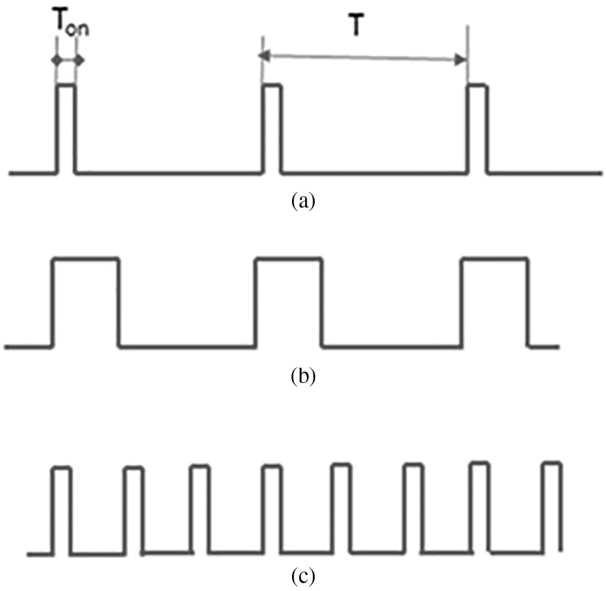

Figure 2. Brightness effect of the strobe light control: (a) low duty ratio, (b) high duty ratio (longer on-time), and (c) high duty ratio (high jetting frequency).

by a strobe light in Figs. 2(b) and (c) are brighter than that obtained by a strobe light in Fig. 2(a).

Figures 3 and 4 show the jetting frequency and the strobe light effects on the brightness of the droplet image. The effects of the jetting frequency are investigated by varying the jetting frequencies at 500 Hz, 3 kHz, 5 kHz, and 10 kHz in our experiment. As shown in Figs. 3 and 4, the droplet image becomes brighter when the jetting frequency increases in the case where a fixed T_{on} is used. A comparison of the image in Figs. 3 and 4 shows that the strobe light on-time, T_{on}, also affects the image brightness. The proper on-time for the strobe light is important because the results of the image analysis may differ according to the brightness of the image. For example, if $T_{on} = 5$ μs is used, the image of the droplet may be too bright for the cases where the jetting frequency is higher than 3 kHz, as shown in Fig. 4. In addition, there will be image blur related to the droplet movement during the on-time of the strobe light. We recommend a short T_{on} of less than 1 μs to reduce the possible droplet image blur due to the movement of the droplet during the LED on-time. However, a short T_{on} due to the low duty ratio of the LED light can result in a dark image in the case with a low jetting frequency. For example, in the case with an on-time of $T_{on} = 0.5$ μs, the brightness of the image is too dark for image analysis if the jetting is reduced to below 3 kHz. In this study, the same image brightness is obtained throughout experiment by using a fixed duty ratio of 0.005, with the equivalent brightness of 0.5 μs at 10 kHz, as shown in Fig. 3(d). As a result, the light on-time, T_{on}, varies according to jetting frequency and increases in the case with a low jetting frequency to achieve the same image brightness. For example, an on-time of $T_{on} = 10$ μs should be used in the case where a jetting frequency of 500 Hz is used, which results in a significant motion-related blur due to the long on-time of the strobe light. We need to use a shorter on-time to reduce the image blur. By considering the image brightness and the droplet image blur, an on-time of $T_{on} = 3$ μs is used in the case with a jetting frequency lower than 500 Hz, which results in a slightly darker image due to the smaller duty ratio of 0.0015. If we assume that the jetting speed is 2 m/s and the on-time of the strobe light is $T_{on} = 3$ μs (or 0.5 μs), the travel distance for the droplet during the on-time is about 6 μm (or 1 μm). This corresponds to an uncertainty (or image blur) of 6 pixels (or 1 pixel) in the image if 1 μm corresponds to 1 pixel in the imaging system. Nonetheless, it is difficult to quantify the error in the image analysis based on the number of blurred pixels because the blurred pixels are mainly observed in the direction of the motion, and the results of the image analysis are also dependent on the threshold that is used to obtain the locations of the edges. The uncertainty in the image analysis is quantified by using the reference mass, which can be considered to be accurate, for comparison. Details will be discussed later.

Note that, in the case with a low jetting frequency, an accurate measurement for the droplet volume is difficult, because the uncertainty in the droplet volume that is related to the image blur increases as a result of the use of a longer T_{on}. Moreover, the droplet image produced with a jetting frequency of less than a few hundred Hz is likely to vary in brightness because the frame rate of the CCD camera used in the visualization system can be as low as 30 fps (frames per second).

A single-event imaging technique and a high-speed camera can be effectively used for uniform lighting conditions irrespective of the jet frequencies.[3,9–11] In the single-event imaging technique, both the high-intensity flash light and the CCD camera are synchronized with respect to the jet signal such that each droplet image is captured using a single firing pulse. However, the method may require additional algorithms to obtain the average droplet volume over a long period of time.

Figure 3. Image brightness according to a jetting frequency of $T_{on} = 0.5$ μs.

(a) 500 Hz (b) 3 kHz (c) 5 kHz (d) 10 kHz

Figure 4. Image brightness according to a jetting frequency of $T_{on} = 5$ μs.

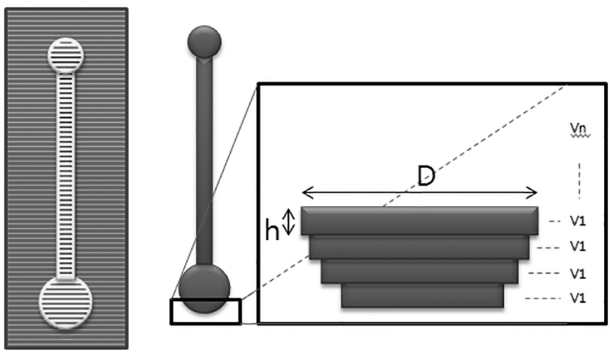

Figure 5. Schematic of the image analysis used to measure the droplet volume.

In this study, we do not have an image brightness variation issue in measuring the droplet mass accurately because the jetting frequency of interest was above 1 kHz. To obtain the same image brightness, the same duty ratio of LED light was used irrespective of the jetting frequency. Furthermore, an additional averaging algorithm is not required due to the inherent averaging characteristics of strobe visualization.

Image Analysis Algorithm for the Droplet Volume

As shown in Figs. 3 and 4, most of the droplet images may not be spherical in shape. The droplet volume of a non-spherical droplet image is measured with a set of one-dimensional horizontal region of interest (ROI) lines that are equally spaced along the droplet in order to detect the edges of the droplet images, as illustrated in Figure 5.[1,3,8,12]

The two detected edges are used to calculate the droplet volume as

$$V = \sum_{i=1}^{n} V_i \quad \text{and} \quad V_i = \pi \left(\frac{D_i}{2} \right)^2 h. \tag{1}$$

Here, the distance between the horizontal edges, D_i, is different according to the size of the edges (droplet size), while the vertical lines are equally spaced at a pre-determined distance, h. Here, the subscript, i, is the sliced volume element number, and n is the number of sliced elements.

For better accuracy, it has been reported that truncated cones may result in better accuracy than right cylinders.[13]

The use of a vision-based volume measurement has an advantage in that the speed of the measurement is much faster and is less affected by ink evaporation when compared to the mass measurement method. However, it has drawbacks in that the volume of the droplet may be affected by the imaging conditions, such as the brightness of the image and the threshold value that is required for either the binary image conversion or edge detection. As a result, there might be errors of up to 10%, unless the imaging conditions are properly controlled.[2]

As a result, a careful image calibration process is required in order to increase the accuracy of the measurement of the droplet volume. The calibration process requires a reference droplet volume (or mass) that can be considered to be accurate. In this study, a droplet mass measured with a microbalance is proposed to obtain the reference mass (volume). In order to allow for a direct comparison with the mass of the reference droplet, the droplet volume is converted to mass by using the density of the fluid. To this end, we take 10 ml of the jetting fluid to measure the corresponding mass in order to calculate the density.

Droplet Mass Measurement

This section discusses the methods that are used to measure the mass of the droplet using the microbalance. It is important to understand the effects of the jetting frequency on the accuracy of the measurement, and for this purpose jetting frequencies of 500 Hz, 3 kHz, 5 kHz, and 10 kHz were used to deposit ink on the microbalance.

For the in-situ mass measurement, a time interval of 1 s was used to obtain the mass data from the microbalance. The collected droplet mass data can be fitted to a regression line with respect to time, t, as

$$y = a^* t + b. \tag{2}$$

Here, a is the slope of the curve-fitted mass data, and b is the initial mass. In this study, the initial mass was set to zero for convenience, and then the uncompensated droplet mass, M_u, can be calculated by dividing the slope with the jetting frequency in Hz, f, as

$$1 \text{ droplet mass } (M_u) = a/f. \tag{3}$$

The use of the fitted data with Eq. (2) has advantages in calculating the droplet mass since the mass increase rate, a, can be calculated as the data are collected, and thereby in-situ measurements are possible. In addition, the reliability of the measured mass can be easily verified by using the correlation coefficient. To improve the accuracy of the fitted regression line using Eq. (1), the number of mass data may be increased. However, we do not recommend obtaining more data than

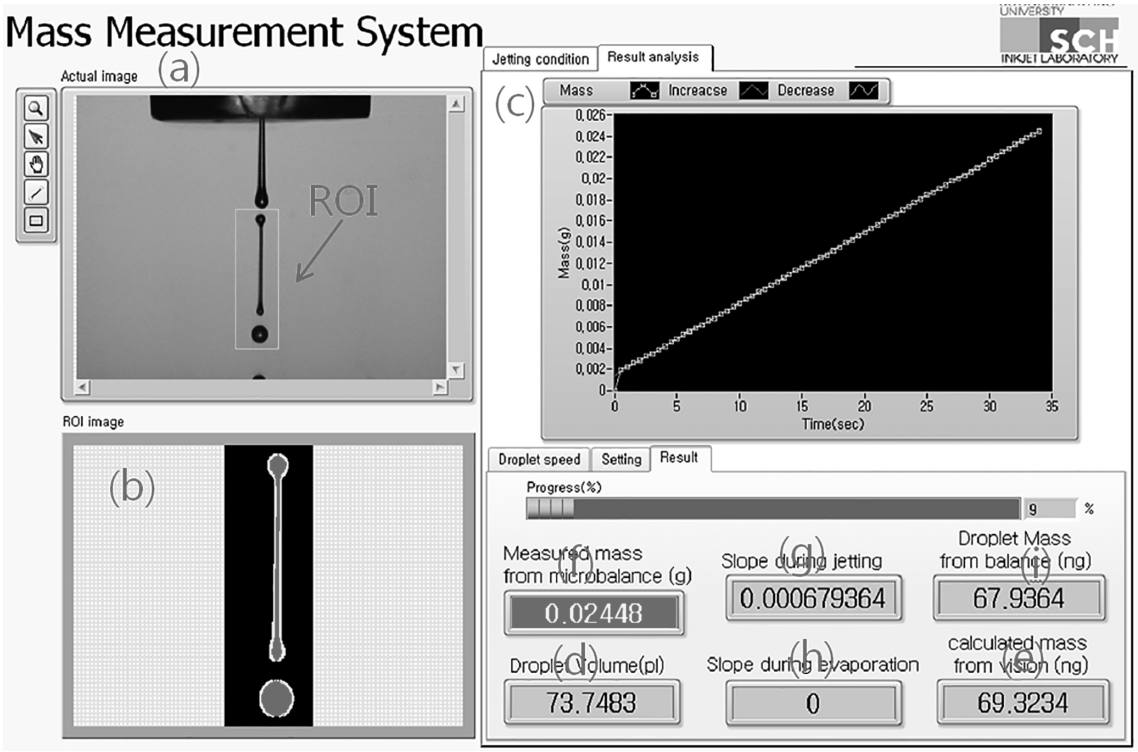

Figure 6. In-situ measurement software for the droplet volume and mass measurement.

necessary, because this would result in a slow measurement. The amount of data can be reduced in order to reduce the time required to measure the droplet if the slope has sufficient linearity with a correlation coefficient greater than 0.9.

Note that the result for the mass measurement using Eq. (3) is accurate only when the effect of the evaporation is negligible. However, the effect of the evaporation often cannot be neglected, and a compensation algorithm should be used to take account of the evaporation. To evaluate the evaporation effect, we measure the mass decrease rate during the non-jetting condition after jetting has stopped.

To this end, the mass data during the non-jetting condition were collected at intervals of 1 s to calculate the evaporation rate by using a linear regression as

$$Y = c^{*}t + d. \tag{4}$$

Normally, the slope of the mass data for the evaporation measurement, c, has a negative value, since the mass on the microbalance decreases with respect to time. Here, d is the initial mass at a time when the jetting stopped to measure the effect of the evaporation. When we assume that the same effect exists in the jetting region, the compensated droplet mass, M_c, can be calculated as

$$1\text{drop mass } (M_c) = (a - c)/f. \tag{5}$$

The compensation method is used to correct the measurement errors due to evaporation. The measurement algorithm using Eqs. (3) and (5) is implemented in our in-situ measurement software, which will be discussed later.

Note that the evaporation rate on the microbalance, c, may differ according to the amount of droplets that are placed on the microbalance. As a result, nonlinear behavior with respect to time is often observed if the amount of ink on the microbalance varies significantly during jetting. The measurement for the uncertainty increases when ink with a low boiling temperature is used, which evaporates quickly. The droplets might be pre-jetted on the microbalance prior to measurement to reduce the nonlinear evaporation effect. However, in the case where fast-drying ink is used, the evaporation rate of the pre-jetted ink on the microbalance, c, could exceed the mass increase rate, a, on the microbalance during jetting. Therefore, pre-jetting was not considered in this study prior to the mass measurement.

In-situ Measurement of the Droplet Mass and Volume

Figure 6 shows the in-house (laboratory) in-situ measurement software for droplet volume and mass. Fig. 6(a) shows the droplet image acquired using the drop visualization system while the droplet is jetted from the head of the inkjet. The image analysis is focused on the target droplet by defining an ROI. Fig. 6(b) shows the image extracted within the ROI. The image within the ROI is analyzed by converting the gray image to a binary image, and then an edge detection technique is used to obtain the volume of the droplet, as illustrated in Fig. 5. In this study, we used a binary image to detect the edges instead of a grayscale image because morphology functions can easily remove unwanted particles from the binary image.[12] Eq. (1) is used to calculate the droplet volume, as shown in Fig. 6(d). Then, the droplet

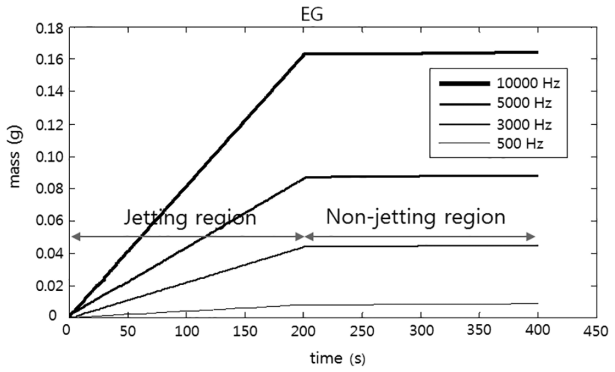

Figure 7. Mass measurement results for the EG.

volume is converted to droplet mass by using the density of the ink, as shown in Fig. 6(e), which will be compared to the droplet mass that is measured using the microbalance in Fig. 6(i). The weight data in Fig. 6(f) are acquired once a second from the balance via serial communications, and the mass data that are collected are then plotted in a graph, as shown in Fig. 6(c). The plotted data are used to fit the regression line in Eq. (2) using a least squares method. From the fitted line, the slope for the mass, which corresponds to a in Eq. (2), increases and can be calculated as shown in Fig. 6(g). Then, the slope is divided by the jetting frequency to obtain the mass for one droplet shown in Fig. 6(i). The mass will be compensated by using the mass decrease slope shown in Fig. 6(h), which is obtained by obtaining an additional fitted regression line for the mass data with a non-jetting condition based on Eq. (4). Then, the compensated droplet mass in Fig. 6(i) will be updated by using Eq. (5). To better understand this process, an online video sequence can be viewed.[14]

EXPERIMENTAL RESULTS

The effects of the evaporation are investigated by using several inks with different boiling points, such as when ethylene glycol (EG), isopropyl alcohol (IPA), and a mixture of EG and IPA are used for the jetting material.

Ethylene Glycol (EG)

Mass Measurement Using Microbalance

The density of the EG (Duksan, South Korea) is measured as 1.1083 g/mL at room temperature. The boiling temperature of the EG is about 197°C. The mass of the inkjet droplet is measured by continuously jetting for 200 s. Then, jetting stops and the mass is measured for another 200 s in non-jetting conditions. Note that the initial mass on the microbalance was set to zero since the amount of EG on the microbalance is initially zero.

Figure 7 compares the droplet mass data that were measured using different jet frequencies. Two different regions can be observed, namely a jetting region (0–200 s) and a non-jetting region that was used to measure evaporation (200–400 s). In the case with EG, the data of the mass for the non-jetting condition (200–400 s) remain almost the same throughout the measurement time, indicating that evaporation was negligible. During jetting, the mass increase rate (slope of the graph) increases as the jetting frequency increases. Note that the slope may not be directly proportional to the jetting frequency since the droplet amount (volume) can differ significantly depending on the jetting frequency.[4]

Table I. Droplet mass calculation using regression lines (EG).

	500 Hz	3 kHz	5 kHz	10 kHz
Mass increase rate, a (mg/s)	0.04	0.22	0.423	0.81
Evaporation rate, c (mg/s)	0.00029	0.00034	0.00048	0.0006
Uncompensated mass, $M_u = a/f$ (ng)	80.0	73.3	84.6	81.0
Compensated mass, $M_c = (a - c)/f$ (ng)	79.42	73.22	84.5	80.94

The mass data shown in Fig. 7 can be curve-fitted to two regression lines for both the jetting and non-jetting regions. Table I summarizes the curve-fitted results. Here, the mass measured for the EG droplet can be considered to be accurate because the mass data of all of the jetting frequencies that are shown in Fig. 7 show good linearity, and the evaporation rate, c, is relatively low compared to the increase in the mass rate, a, during jetting.

Note that the mass increase rate for jetting at 500 Hz is about 0.04 mg/s, which may not be sufficiently large considering that the microbalance has a repeatability of 0.03 mg. However, we increased the accuracy of the measurement by collecting mass data for over 200 s, which results in sufficient differences that can be measured using the commercial microbalance. The accuracy of the measurement increases according to the increase in the jet frequency because the amount of mass deposited on the balance increased accordingly.

In the particular case where EG was used, the evaporation was negligible. Note that the slope of the curve-fitted mass data during non-jetting even has a positive value, which may not indicate an actual mass increase. One of the possible reasons for obtaining a positive slope is that it is related to the inherent measurement drift in the microbalance. Assuming that the same effect exists throughout the experiment, including during jetting, the drift can be eliminated by subtracting the drift-related slope, c, from the mass increase slope, a, to obtain the compensated mass, M_c, using Eq. (5).

Droplet Volume Measurement

For comparison, the droplet volume is measured by using a visualized droplet image. Then, the droplet volume is converted to its equivalent droplet mass by multiplying it with the density of EG.

Figure 8 shows the jetting image of the EG acquired using our visualization system according to the jetting frequency. As seen in Fig. 8(d), the use of the ROI is important in the presence of many subsequent droplets in the image. The droplet within the ROI was analyzed in order

Figure 8. Droplet jetting image for EG at different jetting frequencies: (a) 500 Hz, (b) 3 kHz, (c) 5 kHz, (d) 10 kHz .

Table II. Comparison of the EG droplet amounts measured by using the visual system and the microbalance.

Frequency	500 Hz	3 kHz	5 kHz	10 kHz
Droplet mass calculated from volume, $VM_v = \rho^* V$ (ng)	77.0	71.9	83.3	81.4
Difference without mass compensation (%) $(M_u - M_v)/M_v^*100$	3.90	1.99	1.56	−0.49
Difference with mass compensation (%) $(M_c - M_v)/M_v^*100$	3.14	1.84	1.45	−0.57

to calculate the droplet volume based on the edge detection method, as illustrated in Fig. 5.

Since the results of the measurement may have accuracy issues due to the various imaging conditions, such as image resolution, lens focus, and threshold value, the imaging system needs to be calibrated to increase the accuracy of the measurement.

The amount (mass) of the reference droplet must be measured under the same conditions to calibrate the imaging system. For this purpose, the droplet mass measured at a frequency above 5 kHz was used as the reference mass since the measurement can be considered to be accurate due to the large amount of deposition on the microbalance. Then, the imaging conditions (such as the threshold value for the edge detection, the camera setup, and the lens focus) are adjusted such that the difference between the measured droplet volume and the reference mass can be within 2%, which is an accuracy that is practically achievable by using our current experimental setup.

Table II shows a comparison of the results for the mass of the droplet calculated using visual imaging (Fig. 8) and the measured mass data (Fig. 7). As shown in Table II, the difference in the amount measured for the droplet using the two different methods remains within 2% if the jetting frequency is above 3 kHz. Note that the uncertainty in the measurement of the volume increases if the jetting frequency is low. A trade-off between image brightness and image blur due to the movement of the droplet is the main cause of the larger uncertainty in the measurement. The experimental results in Table II indicate that the uncertainty increases from 1.45% to 3.14% if the jetting frequency is reduced from 5 kHz to 500 Hz, if the mass measurement for the EG is assumed to be accurate.

IPA (Isopropyl Alcohol)

Mass Measurement Using Microbalance

The boiling temperature of IPA is about 82.6°C, which is considerably lower than that of EG. Figure 9 shows the results for the mass measurement of IPA, where the effect of the evaporation can be clearly observed during non-jetting (200–400 s).

In the case of a jetting frequency lower than 500 Hz, the mass of the droplet could not be measured by using the microbalance because the amount remaining on the microbalance was very small due to quick evaporation of the jetted droplet.

The mass data shown in Fig. 9 are fitted to the corresponding regression lines. Table III shows the slope of the mass increase (or decrease) rate that was calculated for the regression lines. The slope and jetting frequency are used to calculate the mass of the droplet, as shown in Table III.

Note that the evaporation rate measured for the non-jetting condition (200–400 s) is different depending on the jetting frequency that is used. For example, the mass evaporation rate increased from 0.138 mg/s to 0.347 mg/s when the jetting frequency increased from 3 kHz to 10 kHz. In both cases, the mass increase rate, a, during jetting is higher than the mass evaporation rate, c, during non-jetting. However, in the case of 5 kHz, the evaporation rate (0.249 mg/s) is similar to that the mass increase rate during jetting (0.24 mg/s). The evaporation of IPA was complex and presented a nonlinear behavior. Our experimental results indicate that the surface area (or droplet amount) of the deposited ink was related to the evaporation behavior.

In the case where ink with a low boiling temperature is measured, the mass of the measured droplet with or without compensating for the evaporation exhibits a significant difference, as shown in Table III. The uncompensated mass of the droplet, M_u, was underestimated because a significant fraction of the ink deposited on the microbalance evaporated during jetting. On the other hand, the accuracy of the compensated mass, M_c, needs to be validated. In this study, a calibrated imaging system was used to validate the mass measurement in the presence of evaporation.

Droplet Volume Measurement

Figure 10 shows a visualization of the droplet image with IPA. As shown in Fig. 10, the jetted droplet has a satellite with a long ligament. The satellite behavior is known to be related to the properties of the ink and the driving waveform.[8] In the case with high-frequency jetting, the main droplet,

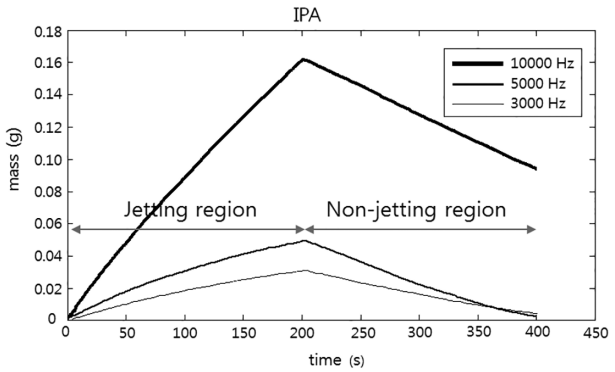

Figure 9. Mass measurement results for IPA.

Table III. Droplet mass calculation using the corresponding regression lines (IPA).

Frequency	3 kHz	5 kHz	10 kHz
Mass increase rate, a (mg/s)	0.15	0.24	0.79
Mass decrease rate, c (mg/s)	−0.138	−0.249	−0.347
Droplet mass without compensation (ng) $M_u = a/f$	50.0	48.0	79.0
Droplet mass with compensation (ng) $M_c = (a - c)/f$	96.0	97.8	113.7

(a) (b) (c)

Figure 10. Droplet jetting images of IPA with different jetting frequencies: (a) 3 kHz, (b) 5 kHz, (c) 10 kHz.

(a) (b) (c)

Figure 11. Detected edges of the jetted IPA droplets within the ROIs: (a) 3 kHz, (b) 5 kHz, (c) 10 kHz.

the satellites, and the subsequent droplets are likely to be close to one another, as seen in Fig. 10(c). Figure 11 shows droplet images within the ROI that are used to calculate the volume of the target droplet according to edge detection, as illustrated in Fig. 5.

The droplet volume that was calculated is converted to droplet mass by using the density of the IPA, which was measured as $\rho = 0.775$ g/ml. Then, the droplet mass that was measured using the microbalance can be directly compared to the droplet mass calculated by using the vision-based method.

Table IV shows a comparison of mass measurement and vision measurement results. As shown in Table IV, the difference could be of up to 50% in the case where the mass is uncompensated since the mass increase slope, a, during jetting was similar to the mass decrease rate, c, during non-jetting for jetting frequencies of 3 kHz and 5 kHz, as shown in Table III. Eq. (5) can be used to compensate for the effect of the evaporation, and the uncertainty in the measurement can be reduced to a small percentage. For example, the difference in the measurement is reduced to 2.14% and 0.96% from 46.8% and 50.45% for the case with frequencies of 3 kHz and 5 kHz, respectively, as shown in Table IV.

Table IV. Comparison of the IPA droplet amounts measured by using the vision and microbalance methods.

Frequency	3 kHz	5 kHz	10 kHz
Droplet mass calculated from volume, $VM_v = \rho^* V$ (ng)	93.99	96.87	113.11
Difference without Evaporation compensation (%), $M_u = (M_u - M_v)/M_v$	46.80	−50.45	−30.16
Difference with Evaporation compensation (%) $M_c = [(M_c - M_v)]/M_v$	2.14	0.96	0.52

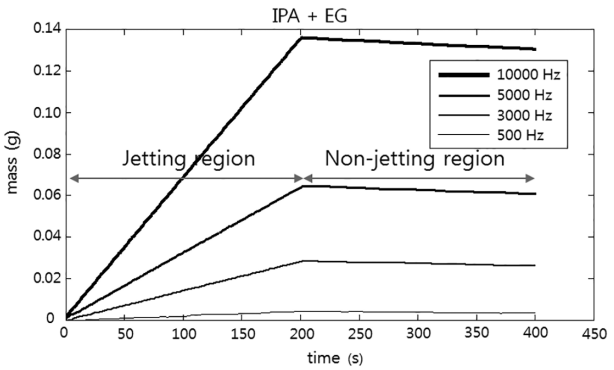

Figure 12. Mass measurement results for mixed IPA and EG ink.

Mixed IPA and EG Ink

Mass Measurement Using Microbalance

Subsequently, mixed IPA (50 wt%) and EG (50 wt%) ink was used as the jetting material to investigate the effects of the evaporation on the mass measurements. As seen in Figure 12, the effect of the evaporation can be clearly observed in the non-jetting region (200–400 s) due to the IPA content. When compared to the mass measurement results for pure IPA shown in Fig. 9, the increase and decrease in the slopes of the mass data exhibit linear behavior with respect to time.

Table V shows the droplet mass calculated by using fitted regression lines for the mass data. In the case with jetting at a frequency of 10 kHz, the evaporation rate of the mixed ink is about 0.275 mg/s, which is much less than that of pure IPA at 0.347 mg/s. As previously discussed, the evaporation rate is dependent on the jetting frequency. For example, the mass evaporation rate in the non-jetting condition (200–400 s) increases from 0.004 mg/s to 0.0275 mg/s when the jetting frequency in the jetting region (0–200 s) increases from 500 Hz to 10 kHz.

Figure 13. Droplet images for the mixed ink with IPA and EG: (a) 500 Hz, (b) 3 kHz, (c) 5 kHz, (d) 10 kHz.

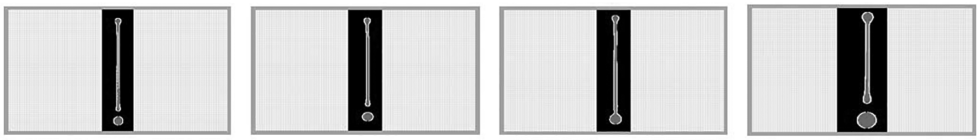

Figure 14. Detected edges of jetted droplet of the mixed ink within the ROI: (a) 500 Hz, (b) 3 kHz, (c) 5 kHz, (d) 10 kHz.

Table V. Droplet mass calculation using regression lines of the mass data of the mixed (IPA and EG) ink.

Frequency	500 Hz	3 kHz	5 kHz	10 kHz
Mass increase rate, a (mg/s)	0.022	0.14	0.32	0.670
Mass decrease rate, c (mg/s)	−0.0040	−0.0118	−0.019	−0.0275
Droplet mass without evaporation compensation, $M_U = a/f$ (ng)	44.0	46.67	64.0	67.0
Droplet mass with evaporation compensation, $M_C = (a - c)/f$ (ng)	52.0	50.6	67.8	69.75

Table VI. Comparison of the droplet amount of the mixture fluid measured using the vision and microbalance systems.

Frequency	500 Hz	3 kHz	5 kHz	10 kHz
Droplet mass calculated from volume, $VM_V = \rho * V$ (ng)	58.75	51.12	68.34	69.55
Difference without compensation (%) $(M_U - M_V)/M_V$	−25.11	−8.71	−6.35	−3.67
Difference with compensation (%) $(M_C - M_V)/M_V$	−11.49	−1.02	−0.79	0.29

The curve-fitted regression lines for both the jetting and non-jetting regions can be used to calculate the droplet mass, M_c, as shown in Table V. Note that the difference between the compensated mass, M_c, and the uncompensated mass, M_u, becomes smaller as the jetting frequency increases, indicating that the measured mass is less affected by evaporation when using a higher jetting frequency. The mass of the droplet that was measured is then validated by using the droplet volume measured using the vision-based technique.

Droplet Volume Measurement

Figure 13 shows the jetting image of the mixed ink with respect to the jet frequency. Figure 14 shows the edge that is detected for the droplet images within the ROIs to calculate the droplet volumes. As previously discussed, calibrated imaging conditions are used to calculate the droplet volume. In the case with high-frequency jetting, as shown in Fig. 13(d), the ROI should be carefully selected to focus on the target droplet while excluding subsequent droplets from the image analysis. Then, the droplet volume, V, is calculated and converted to the droplet mass, M_v, as shown in Table VI. The converted droplet mass can be used as reference data to validate the mass measurement results shown in Table V.

A comparison of the non-compensated droplet mass with the calibrated droplet volume allows us to understand that the accuracy of the mass measurement is reduced as the jetting frequency decreases, as shown in Table VI. In contrast, the accuracy of the measurements increases when using the proposed compensation method based on Eq. (5). Assuming that the image analysis using the calibrated imaging conditions is reasonably accurate, the uncertainty of the measured droplet mass at above 3 kHz can be reduced to be as low as 1%. However, the uncertainty of the mass measurement for the case at 500 Hz is as high as 11.49%, despite compensating for the evaporation.

CONCLUSIONS AND DISCUSSION

An in-situ droplet mass measurement method is presented. The volume of the droplet is simultaneously measured using a vision-based system. To increase the accuracy of the vision measurement, the imaging system was calibrated by using a reference mass measured with the microbalance. In comparison to the measured droplet mass of EG, which is considered to be accurate due to its low level of evaporation, the calibrated droplet volume obtained with our experimental setup was shown to have an uncertainty of less than 2% (or 3%) in the case where the frequency is higher than 3 kHz (or 500 Hz). The use of a vision system to measure the size of the droplet has advantages from a practical point of view in that the accuracy of the measurement is affected less by evaporation. In addition, the measurement time is significantly short compared to mass measurement.

The jetting frequency was shown to be one of the most important parameters when measuring the amount of the droplet with both the microbalance and the droplet visualization methods. The mass measurement with low-frequency jetting below a few hundred Hz was likely to be less accurate as a result of the smaller amount that was deposited on the microbalance. The droplet volume measured with the droplet image is also affected by the jetting frequency because the brightness of image can be affected by the jetting frequency. Uniform image brightness can be obtained by using the same duty ratio of the strobe light. However, the same duty ratio often results in a longer on-time for the strobe light in the case with low-frequency jetting, and image blur occurs as a result of the droplet movement during the on-time of the strobe light.

Evaporation significantly affects the mass measurement if the ink has a boiling temperature lower than 100°C. The evaporation behavior is quite complex and can be dependent on the exposed droplet surface area and mass on the microbalance. Without proper compensation, the measured mass can be underestimated in the presence of significant evaporation. To increase the accuracy of the measurements, we implemented a compensation method based on fitted regression lines for the jetting and non-jetting mass data with respect to time. The proposed compensated method can be used to reduce the uncertainty of the mass measurement with 3 kHz jetting for IPA to 2.14% from an uncertainty of 46.8%.

ACKNOWLEDGMENT

This work was supported by the Mid-career Research Program through an NRF grant, funded by the MEST (NRF-2013R1A2A2A01004802), and was partially supported by the Soonchunhyang University Research Fund.

REFERENCES

[1] K.-S. Kwon, "Vision monitoring," *Inkjet-Based Micromanufacturing*, edited by J. G. Korvink, P. J. Smith and D.-Y. Shin (Wiley-VCH Verlag GmbH & Co. KGaA, Weinheim, Germany, 2012), doi: 10.1002/9783527647101.ch9.

[2] K. S. Kwon, "Speed measurement of ink droplet by using edge detection techniques," Measurement **42**, 44–50 (2009).

[3] I. M. Hutchings, G. D. Martin, and S. D. Hoath, "High speed imaging and analysis of Jet and drop formation," J. Imaging Sci. Technol. **51**, 438–444 (2007).

[4] K. S. Kwon, M. H. Jang, H. Y Park, and H. S. Ko, "An inkjet vision measurement technique for high frequency jetting," Rev. Sci. Instrum. **85**, 065101 (2014).

[5] R. M. Verkouteren and J. R. Verkouteren, "Inkjet metrology: High-accuracy mass measurements of microdroplets produced by a drop-on-demand dispenser," Anal. Chem. **81**, 8577–8548 (2009).

[6] H. Zhuang, P. Lu, S. P. Lim, and H. P. Lee, "Study of evaporation of colloidal suspension droplets with quartz crystal microbalance," Langmuir **24**, 8373–8378 (2008).

[7] D. J. Maloney, G. E. Fasching, L. O. Lawson, and J. F. Spann, "An automated imaging and control system for the continuous determination of size and relative mass of single compositionally dynamic droplets," Rev. Sci. Instrum. **60**, 450 (1989).

[8] K. S. Kwon, "Experimental analysis of waveform effects on satellite and ligament behavior via in situ measurement of the drop-on-demand drop formation curve and the instantaneous jetting speed curve," J. Micromech. Microeng. **20**, 115005 (2010).

[9] H. Dong and W. W. Carr, "An experimental study of drop-on-demand drop formation," Phys. Fluids **18**, 072102 (2006).

[10] S. D. Hoath, O. G. Harlen, and I. M. Hutchings, "Jetting behaviour of polymer solutions in drop-on-demand inkjet printing," J. Rheol. **56**, 1109–1127 (2012).

[11] S. Jung, S. D. Hoath, G. D. Martin, and I. M. Hutchings, "A new method to assess the jetting behaviour of drop-on-demand inkjet fluids," J. Imaging Sci. Technol. **55**, 010501 (2011).

[12] K. S. Kwon and S. Ready, *Practical Guide to Machine Vision Software: an introduction with LabVIEW* (Wiley-VCH, Germany, 2015).

[13] A. V. D. Bos, M.-J. V D Meulen, T. Driessen, M. V. D. Berg, H. Reinten, H. Wijshoff, M. Versluis, and D. Lohse, "Velocity profile inside piezoacoustic inkjet droplets in flight: comparison between experiment and numerical simulation," Phys. Rev. Appl. **1**, 014004 (2014).

[14] K. S. Kwon, Inkjet droplet mass measurement, online: http://youtu.be/50P3Jn4xwAs (2015).